

AD A138 382

POROUS ELECTRODES I: NUMERICAL SIMULATION USING RANDOM
NETWORK AND SINGLE PORE MODELS(U) BROOKLYN COLL NY DEPT
OF PHYSICS M KRAMER ET AL. 31 JAN 84 TR 5

1/1

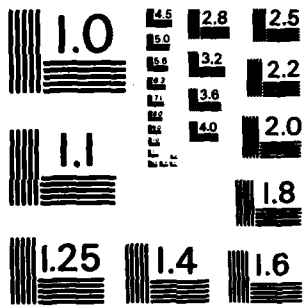
UNCLASSIFIED

N00014-81-K-0399

F/G 12/1

NI

END
DATE
FILED
3 84
DT-1



MICROCOPY RESOLUTION TEST CHART
NATIONAL BUREAU OF STANDARDS-1963-A

OFFICE OF NAVAL RESEARCH

Contract N00014-81-K-0399

Task No. NR - 628-765

TECHNICAL REPORT NO. 5

AD A138382

POROUS ELECTRODES I: NUMERICAL SIMULATION USING RANDOM NETWORK
AND SINGLE PORE MODELS

by

Michael Kramer and Micha Tomkiewicz

Accepted for Publication

in

Journal of the Electrochemical Society

Physics Department, Brooklyn College of CUNY
Brooklyn, N. Y. 11210

January, 1984

Reproduction in whole or in part is permitted for
any purpose of the United States Government

This document has been approved for public release
and sale; its distribution is unlimited

DTIC
ELECTE
FEB 29 1984

A

DTIC FILE COPY

84 02 22 099

REPORT DOCUMENTATION PAGE		READ INSTRUCTIONS BEFORE COMPLETING FORM
1. REPORT NUMBER 5	2. GOVT ACCESSION NO. AD-A138 382	3. RECIPIENT'S CATALOG NUMBER
4. TITLE (and Subtitle) POROUS ELECTRODES I: NUMERICAL SIMULATION USING RANDOM NETWORK AND SINGLE PORE MODELS		5. TYPE OF REPORT & PERIOD COVERED
7. AUTHOR(s) MICHAEL KRAMER MICA TOMKIEWICZ		6. PERFORMING ORG. REPORT NUMBER
9. PERFORMING ORGANIZATION NAME AND ADDRESS PHYSICS DEPARTMENT BROOKLYN COLLEGE OF CUNY		8. CONTRACT OR GRANT NUMBER(s) N00014-81-K-0399
11. CONTROLLING OFFICE NAME AND ADDRESS OFFICE OF NAVAL RESEARCH /CHEMISTRY ATTN: CODE 413, 800 N. QUINCY STREET ARLINGTON, VA. 22217		10. PROGRAM ELEMENT, PROJECT, TASK AREA & WORK UNIT NUMBERS NR-628-765
14. MONITORING AGENCY NAME & ADDRESS (if different from Controlling Office)		12. REPORT DATE JANUARY 31, 1984
		13. NUMBER OF PAGES 26
		15. SECURITY CLASS. (of this report) UNCLASSIFIED
		15a. DECLASSIFICATION/DOWNGRADING SCHEDULE
16. DISTRIBUTION STATEMENT (of this Report) APPROVED FOR PUBLIC RELEASE AND SALE. DISTRIBUTION UNLIMITED		
17. DISTRIBUTION STATEMENT (of abstract entered in Block 20, if different from Report)		
18. SUPPLEMENTARY NOTES ACCEPTED FOR PUBLICATION IN THE JOURNAL OF THE ELECTROCHEMICAL SOCIETY		
19. KEY WORDS (Continue on reverse side if necessary and identify by block number) ELECTRODE, IMPEDANCE, BATTERY, TOPOGRAPHY		
20. ABSTRACT (Continue on reverse side if necessary and identify by block number) → A Random Network model is introduced to stimulate the porous metal-electrolyte interface. This is the first time that an attempt has been made at defining a model for this system that maintains the random nature of the rough topology. A previously utilized model for this system - the single pore model is explored and extended. The models are compared, and the results of the Random Network model are found to be in qualitative agreement with the single pore models.		

DD FORM 1473
1 JAN 73EDITION OF 1 NOV 65 IS OBSOLETE
S/N C102 LF-014-6601

SECURITY CLASSIFICATION OF THIS PAGE (When Data Entered)

B2IC
COPY
RESTRICTED
2

AI

SECURITY CLASSIFICATION OF THIS PAGE (When Data Entered)

**POROUS ELECTRODES I:
Numerical Simulation Using Random Network
and Single Pore Models**

by
Michael Kramer
and
Micha Tomkiewicz

Department of Physics
Brooklyn College of CUNY
Bedford Avenue and Avenue H
Brooklyn, N.Y. 11210

ABSTRACT

A Random Network model is introduced to simulate the porous metal-electrolyte interface. This is the first time that an attempt has been made at defining a model for this system that maintains the random nature of the rough topology. A previously utilized model for this system - the single pore model is explored and extended. The models are compared, and the results of the Random Network model are found to be in qualitative agreement with the single pore models.

Keywords: Electrode Impedance Battery Topography

INTRODUCTION

The porous metal electrode is a subject of intense theoretical and applied interest. Although widely utilized in electrochemical systems, especially in battery technology, very little is known in detail about the porous interface from first principles, aside from a general knowledge of how the porous electrode's behavior deviates from flat-electrode behavior. Specifically, it would be useful to know how the complicated topology of the porous metal electrode contributes to the electrical properties of the interface. Previous attempts at modeling the porous electrode are presented in the review article by DeLevie [1]. The macroscopic model [2] treats the electrode-electrolyte system as a superposition of two continua, one of the electrode matrix and one of the solution matrix that fills all the unoccupied space. The solution is assigned an effective conductivity, and the interface is considered to have an effective capacitance per unit area. The single pore model is based on a one-dimensional representation of a pore as a transmission line (see figure 5) which represents a pore of "average pore length". These models, however, do not account for the random distribution of pores in a true porous solid, nor for a complicated surface topology. We have chosen to introduce a three dimensional model of the rough interface based on the random-network lattice that has proven to be so useful in representing conduction in inhomogeneous materials and related percolation problems [3,4,5]. A.c. impedance measurements are widely used experimentally for the in-situ characterization of electrochemical systems under equilibrium conditions. In conducting these measurements on porous electrodes, the complex topology of the electrode in various states of charge yields ambiguous data, not subject

to a unique interpretation. The computer simulation allows us to examine the impedance of the system as a function of given charge accumulation modes at the electrode-electrolyte interface. The model is not intended to portray the d.c. operation of the electrode, but rather to provide a means for understanding the interface. Using an IBM/370 computer, we construct our model and calculate its complex impedance, $Z(\omega)$, in the frequency range of one Hertz to one Megahertz. Based on this impedance spectrum, we model the system in terms of passive elements [6].

In this paper, we will present our model in detail, discuss preliminary results, and compare these results with the "DeLevie model". We will also discuss further work being done to utilize this model for a more detailed characterization of the interface.

I. THE "RANDOM" NETWORK MODEL

We consider a simple system, in which a 1 cm³ porous metal electrode is immersed in electrolyte, along with a counter-electrode. Only the bottom (1 cm²) surface of the electrode is exposed to the electrolyte. The electrode is allowed to discharge, allowing for a build-up of a semiconductor on the metal surfaces exposed to the electrolyte. To explore the electrical behavior of this system, we note that we may define a local conductivity, $\sigma(\vec{r})$, the bulk conductivity at point \vec{r} in our system. Rather than attempt to solve for the current distribution using the electrostatic equations for the continuous case, we transform the problem into one requiring the solution of a discrete set of Kirchoff's Law equations (a finite difference approximation to the continuum problem) [3]. We subdivide our bulk system into a regular cubic mesh of points $\{r_i\}$ ($i=1,S$) and assign to each branch of the mesh a conductivity that represents the conductivity of the surrounding bulk in that region of space. Let the conductance of the circuit branch that connects node i and j be denoted as g_{ij} , the voltage at node i be V_i , and the net current into node i be I_i . We then have $(S-1)$ equations of the form:

$$\sum_j g_{ij} (V_i - V_j) = I_i \quad (1)$$

or in matrix notation:

$$G \cdot V = I$$

where G is the conductance matrix ($G_{ii} = \sum_j g_{ij}$ and $G_{ij} = -g_{ij}$), V is a vector containing the voltages on each node with respect to ground, and I is a vector containing the net current inputs to each node. We may solve these simultaneous equations for the V 's on all the nodes,

and for the total impedance of the system. A detailed presentation of the algorithm that we have employed follows.

We define a three dimensional cubic lattice, $A(i,j,k)$, where i, j and k range from 1 to N , and $N^3=S$, the total number of nodes. N is chosen so that it is sufficiently large to approximate an infinite system. Construction of the electrode is simulated using a random number generator to place "metal" at various points in the lattice, until the desired porosity is reached. A check is made of the resulting electrode to insure that it is continuous and that no pieces of metal are "hanging" in mid-air. Any disjointed pieces of metal are removed, and are randomly replaced on the remaining available lattice points. This process is repeated until a continuous electrode of the desired porosity is obtained. Lattice plane $k=1$ is defined as electrolyte, to represent the solution; the electrode itself begins at lattice plane $k=2$. The electrolyte is allowed to "seep into" the pores in the electrode until all accessible pores are filled, by searching for continuous electrolyte paths from the $k=1$ plane throughout the electrode. Any point on the lattice which has been left empty (i.e. no metal was placed there, and electrolyte was precluded from penetrating to that site) is considered to be "air".

Each lattice point represents a node in a three dimensional circuit network (See figure 1), and each pair of nodes defines a circuit branch in the network. The impedance of each branch is determined by the characteristics of the two surrounding nodes. Thus, for example, if $A(1,1,1)$ is electrolyte and $A(1,2,1)$ is also electrolyte, the circuit branch defined by those nodes will consist of two series resistors of resistance R_0 (the resistance of a microscopic section of the

electrolyte). If A(1,1,2) is metal and A(1,2,2) is metal, then the circuit branch defined by those two nodes will be two series resistors of value R_m (the resistance of a microscopic section of the metal). Finally, the branch defined by A(1,1,1) - electrolyte, and A(1,1,2) - metal, is represented by an R_m and an R_e resistor in series, with the addition of a parallel R-C element in series with them to represent the semiconductor-electrolyte interface that results (see Figure 2). Any circuit branches leading into nodes that are defined as "air" are taken to be of infinite resistance.

The values that we have chosen to use as our unit impedances for the individual components of metal, electrolyte, and semiconductor are presented in Figure 2. These values were obtained by taking the values of bulk impedance for a 1 cm³ sized sample, (we chose numbers characteristic of Zn and ZnO) and scaling them down to the magnitude of a unit pore size- approximately 10 μ in diameter. We define a characteristic time constant of the interface, $\tau = R_p C$. These components are assembled into a system, as described above (see figure 3) and the total impedance of the system is calculated. The total impedance is then rescaled by an appropriate factor that normalizes the whole system to a 1 cm³ size. Thus, an attempt is made to obtain impedance data with numbers representative of that which might be encountered in a real system.

Once the electrical network has been defined, the computer sets up the Kirchoff's law equations. Due to the fact that our model includes reactive circuit elements, the quantities G, V, and I in equations (1) are complex, and may be represented as 2S-1 equations of the form:

$$\begin{pmatrix} G_r & -G_i \\ G_i & G_r \end{pmatrix} \begin{pmatrix} V_r \\ V_i \end{pmatrix} = \begin{pmatrix} I_r \\ I_i \end{pmatrix} \quad (2)$$

where the subscripts r and i stand for the real and imaginary components respectively.

A known current is sent uniformly into all the bottom nodes (so as to eliminate the "edge effects" that would result if the current were sent only into one node), and the impedance of the system is calculated between one node on the electrolyte plane (1,1,1) and one node of the top electrode plane (N,N,N) by solving for the V 's on all the nodes.

For a system of $N=15$ (a lattice of size $15 \times 15 \times 15$ with 3375 nodes) there are up to 6748 equations to be solved. This is a formidable computer problem. Indeed, the task would be prohibitive without taking advantage of the fact that the conductance matrix, G , is a sparse-symmetric coefficient matrix.

A number of techniques exist for the solution of this class of problems. A widely used method for solving the simultaneous equations in the Random Resistor lattice is the Gauss Seidel iteration procedure with over-relaxation [5]. This is a very economical method, in both execution time and storage space. A serious drawback of this technique is the relatively strict requirements that it places on the coefficient matrix in order for convergence to be achieved, namely that the matrix be either diagonally dominant, or at least positive definite [7]. For Kirchoff's law problems with purely resistive components, diagonal dominance is assured, since the diagonal elements of the conductance matrix are simply the sum of the off diagonal elements. In our problem, with complex impedances, we find that at frequencies for

which the real conductance approaches the same order of magnitude as the imaginary conductance, the Gauss-Seidel procedure does not converge. This is due to the form of the equation in (2) where there are many more off diagonal elements due to the G_i values. When these imaginary components are large, the matrix is no longer diagonally dominant, nor positive definite.

For most of our computations, we have resorted to the use of a Gaussian elimination routine which takes advantage of both the sparseness and the symmetry of the G coefficient matrix [8]. Only the nonzero elements in the upper half triangle of the matrix are stored, and an efficient pivoting strategy is chosen to minimize non-zero matrix fill during the pivoting and to minimize the number of multiplications required in the solution. In practice, the technique is approximately an order of magnitude more expensive to use than Gauss-Seidel in both speed and storage requirements. The advantage of using the Gaussian elimination technique is that a solution is guaranteed for almost any problem. The solutions obtained from the Gauss-Seidel procedure (in the range in which convergence is reached) are in complete agreement with the results obtained using the modified Gaussian elimination technique.

Figure 3 presents a system constructed with a porosity of 0.30, and the resulting impedance of the system as a function of frequency is plotted in figure 4. We have identified three basic regions of interest in the frequency range spanned by our results. Region I is the low frequency range, in which our system seems to behave as a parallel R-C combination (See figure 4). Region II is in the mid-frequency range, with an impedance spectrum that cannot be represented using passive

elements, and Region III is representative of a series R-C combination. The variation of the impedance data as a function of system size is presented in Figure 5 from size N=5 to N=15. For the results presented here, N=15 was used to ensure proper statistical representation of an infinite system.

II. THE SINGLE-PORE MODEL

It is interesting to compare, at least qualitatively, the results from our three dimensional model with the results obtainable from the single pore model previously mentioned [1].

De Levie, following on the heels of other researchers (Daniel¹-Beck, [9] et. al.), suggested that each pore in a porous electrode may be thought of as having a uniformly distributed electrode and electrolyte resistance throughout its length. As such, the single pore may be modeled as in figure 6a, where R is the resistance per unit length of the electrolyte solution inside the pore, and Z is the impedance of the electrode-electrolyte interface. The current-voltage relationships of this circuit may be expressed as a differential equation and a solution may be obtained for the total impedance of the circuit as [1]:

$$Z_o = (RZ)^{\frac{1}{2}} \coth (\rho L)$$

where R and Z are defined above, $\rho=(R/Z)^{\frac{1}{2}}$, and L is the length of the pore. This is the main, and currently utilized [10], result from this model. The main characteristics of the calculation are: (1) Although flat electrode impedances vary as a function of Z, porous surface impedances will be dependant on $(RZ)^{\frac{1}{2}}$, and (2) the contribution of the electrode surface deep inside the pore is negligible, $1/\rho$ becoming

the characteristic "penetration depth". If $\rho L \gg 1$ the pore behaves like a semi-infinite one.

In order to utilize these results for comparison with the Random Network Model, we must introduce a value for Z , and we must also combine the single pore transmission-line impedances to form a complete rough electrode. The former is accomplished by defining the electrode-electrolyte interface as a standard parallel R-C model, as depicted in figure 6b. We have used the same numerical values for the individual components as those in the Random Network Model (here they are shown already normalized to the 10μ single pore size). As a result,

$$Z = r_s + \frac{R_p}{1 + \omega^2 \tau^2} - j \frac{\omega \tau R_p}{1 + \omega^2 \tau^2} \quad (4)$$

where $\tau = R_p C$. Substituting (4) into (3) and simplifying, we get:

$$Z_o = \sqrt{\frac{R_p}{2}} \frac{e^{2x} - e^{-2x}}{e^{2x} + e^{-2x}} \quad (5)$$

$$\times \left\{ \left[(\beta + \alpha)^{\frac{1}{2}} + \frac{2 \sin 2\theta}{e^{2x} - e^{-2x}} (\beta - \alpha)^{\frac{1}{2}} \right] + j \left[(\beta - \alpha)^{\frac{1}{2}} - \frac{2 \sin 2\theta}{e^{2x} - e^{-2x}} (\beta + \alpha)^{\frac{1}{2}} \right] \right\}$$

where we have defined the following quantities:

$$p = \frac{R_p}{1 + \omega^2 \tau^2}$$

$$\alpha = 1 + \frac{r_s}{p} \quad (6)$$

$$\beta = (\alpha^2 + \omega^2 \tau^2)^{\frac{1}{2}}$$

$$x = L \left(\frac{R}{p} \right)^{\frac{1}{2}} \frac{1}{\sqrt{2\beta}} (\beta + \alpha)^{\frac{1}{2}}$$

$$\theta = L \left(\frac{R}{p} \right)^{\frac{1}{2}} \frac{1}{\sqrt{2\beta}} (\beta - \alpha)^{\frac{1}{2}}$$

A log-log plot of the relationship between Z and f (for a single pore) is presented in figure 7. It is interesting to note the similarity in shape between the impedance spectrum of the single-pore model (even though we are only considering a single pore) and that of our Random Network Model (figure 4). The advantage of considering a single pore at the present stage is that it is the only system for which we have an analytic result (equation 5), which may be used to derive expressions for the impedance in different frequency ranges.

We define three frequency regimes:

(a) The low frequency range ($\omega\tau \ll 1$):

$$\text{Re}(Z_0) = K \quad (7a)$$

$$\text{Im}(Z_0) = K\omega\tau$$

where K (independent of frequency) is given as:

$$K = \sqrt{\frac{RR_p}{p}} \frac{e^{2x} - e^{-2x}}{e^{2x} + e^{-2x} + 2}$$

and x is:

$$x = L (R/R_p)^{\frac{1}{2}}$$

The notable features of equation (7a) are the frequency independence of the Real part and the slope 1 dependence (on the log-log plot) in the imaginary part of the impedance (see region I on figure 7).

(b) The intermediate frequency range ($\omega\tau \gg 1$ but $r_s \omega\tau/R_p \ll 1$):

$$\text{Re}(Z_0) = \text{Im}(Z_0) = \sqrt{\frac{RR_p}{2}} \frac{1}{\sqrt{\omega\tau}} \quad (7b)$$

This results in the slope $-\frac{1}{2}$ line in region II of figure 7.

(c) The high frequency range ($\omega\tau \gg 1$ AND $r_s\omega\tau/R_p \gg 1$):

$$\text{Re}(Z_o) = \sqrt{Rr_s} \tag{7c}$$

$$\text{Im}(Z_o) = \frac{1}{2} \sqrt{\frac{R}{r_s}} \frac{R_p}{\omega\tau}$$

which results in a frequency independent real impedance, and the slope -1 line in the imaginary impedance as can be seen in region III of figure 7.

In addition to the frequency limits, it was also assumed that $R_s/R_p \ll 1$, and that $R > r_s$ by at least an order of magnitude (which is usually the case).

To combine the single pores into a unified metal-electrolyte system, we extend De Levie's model slightly. We define an x-y plane and divide it into N^2 squares, and randomly place a rectangular-width pore on the x-y plane with its length extending in the z direction. The length of the pore, L , is also randomly chosen to be from 1 to N , and the pore width, W , is selected so that there is a Gaussian distribution about $W = 2$ (to prevent a few very wide pores from "taking over" the whole electrode). More random sized pores are randomly placed on the x-y plane until the desired porosity is reached. We may then solve for the total impedance of the system by adding up all the parallel impedances due to the individual pores, using equation (5) to represent the impedance of each pore. The impedances of the non-porous sections of the electrode are also added on to the total impedance.

The results, for a porosity of 0.3 and $N=40$, are presented in figure 8. The criteria for choosing N was based on considerations similar to

those used to choose N in the Random Network model, namely that the results be independent of N and statistically independent of the random number. This phase of the calculation was performed on an IBM PC.

III. DISCUSSION OF RESULTS

There is a qualitative agreement between the Random Network model and the single-pore model. A comparison of the passive elements representation of the two systems (figure 4 and figure 8) also yields order-of-magnitude quantitative agreement. One discrepancy between the two models is the definite shift in the location of the "mid-frequency peak" in Figure 8 as compared to the Random Network and single-pore results. A major difference between the two models in construction, is the fact that in the Random Network the pores interact with each other as in a true porous electrode, while in the De Levie model each pore is kept separate from the others, and is a separate channel. The favorable comparison of the two models would seem to bear out De Levie's assertion that "the disregard of crosslinks [between the pores] presumably does not introduce a significant error [1]. Nevertheless, this can be a useful starting place for an explanation of a discrepancy between the two.

The behavior of the system impedance in the Random Network model may be somewhat inferred from the values of the constituent components that make up the system. The low-frequency (real and imaginary) impedance in figure 4 reflects the values of R_p and C of the unit (semiconductor) interface, although the 300Ω value of $\text{Re}(Z)$ is noticeably lower than the $1K\Omega R_p$. In the high-frequency regime, C dominates, totally shunting out R_p , the only contribution to the Real impedance

being R_o . This provides us with an indication that the total behavior of the porous-metal system may be inferred from the values of the components that make up the complicated surface topography. Our ultimate goal is to generate a detailed picture of the macroscopic interface from the impedance data of the microscopic components that make up the system. This will be considered further in a subsequent paper, along with an exploration of the physical significance of the passive elements model of the entire system.

We will also examine the correlation between the single pore analytic results (in the various frequency limits) and the Random Network model. Only a single porosity has been considered thus far, but an exploration of the Random Network model at different porosities is in order. Although some rough surfaces may exhibit a conduction percolation threshold [11,12], we do not expect to see any classical percolation in our system. This is due to the fact that we have constrained the system to be above the percolation threshold by the requirement that the metal electrode be continuous. We would, however, expect to see some less dramatic system dependence on porosity.

ACKNOWLEDGEMENTS

We would like to express our special gratitude to Dr. Philip E. Seiden from IBM, Thomas J. Watson Research Center for helping us to formulate the Random network problem. We would also like to thank Dr. Itzhak Webman from Exxon, for helpful discussions during the initial phases of the project. This work was supported by the Office of Naval Research under contract N00014-81-K-0339.

REFERENCES

1. R. de Levie in Advances in Electrochemistry and Electrochemical Engineering , Vol. 6, John Wiley Interscience, N.Y (1967) p. 329.
2. J.S. Newman and C.W. Tobias, J. Electrochem. Soc., 109, 1183 (1962).
3. S. Kirkpatrick, Rev. Mod. Phys. 45 , 574 (1973).
4. I. Webman, J. Jortner, and M. H. Cohen, Phys. Rev. B 14 , 4737 (1976).
5. I. Webman, J. Jortner, and M. H. Cohen, Phys. Rev. B 11 , 2885 (1975).
6. M. Tomkiewicz, J. Elech. Soc., 126 , 2221 (1978).
7. Carnahan, Luther, Wilkes, Applied Numerical Methods, Wiley (1969) p. 300.
8. G. E. Forsythe, M. A. Malcom, C. B. Moler, Computer Methods for Mathematical Computations , Prentice Hall, 1977.
9. V.S. Daniel'-Bek, Zh. Fiz. Khim., 22 , 697 (1948).
10. S.A.G.R. Karunathilaka, N.A. Hampson, J. Apl. Electroch. 10 , 357 and 603 (1980).
11. M. H. Cohen, M. Tomkiewicz, Phys. Rev. B, 26 , 7097 (1982)
12. M. H. Cohen, J. K. Lyden, M. Tomkiewicz, Phys. Rev. Lett. 47 , 13 (1981).

LIST OF FIGURES

1. Representation of the 3-D Lattice in terms of Circuit elements. Figure 1b shows our model in terms of a checkerboard pattern of bulk components of metal, electrolyte, semiconductor, and air. Figure 1a depicts our representation of (a corner of) Figure 1b in terms of a network of circuit elements. Z_{sc} is the impedance of the semiconductor layer on the interface (see Figure 2).
2. Equivalent circuits used to represent the microscopic components of the system (metal, electrolyte, semiconductor, etc.).
3. The Random Network lattice used to generate the data for Figure 4. At this porosity of .3, the electrolyte does not fully penetrate the lattice. (Actually, the penetration of the electrolyte into the pores seems to conform to classical percolation theory. At porosities above .35 the liquid starts to penetrate through the electrode).
4. Impedance spectrum from the Random Network model at a single porosity (0.3), and a single random number. Three frequency regimes are identified, and we have modelled two regimes with a simple passive element model. The bars on each curve represent the variations in the data when various random number seeds are used to construct the lattice. For each random number seed, the shape of the impedance spectrum is almost identical.
5. The impedance in the Random Network model as a function of system size. All values are normalized to the impedance of lattice size 15 x 15 x 15 (N=15).

6. The De Levie model of a single pore. Figure (6a) presents the general transmission-line model. (6b) presents the value we have chosen for R, the electrolyte impedance, and our specific model for Z, the electrode-electrolyte interface inside the pore.
7. Impedance spectrum from the DeLevie model - single pore. The sections of the curve labelled (1) are areas in which the Imaginary impedance plot is of slope=1 on the log-log plot, and the impedance in these ranges may be modeled by the two passive elements models shown. The section of the curve labelled (2) has a slope=1/2; See equations 7a - 7c.
8. Impedance data from Delevie model - randomly distributed pores. Porosity = 0.3, N=40.

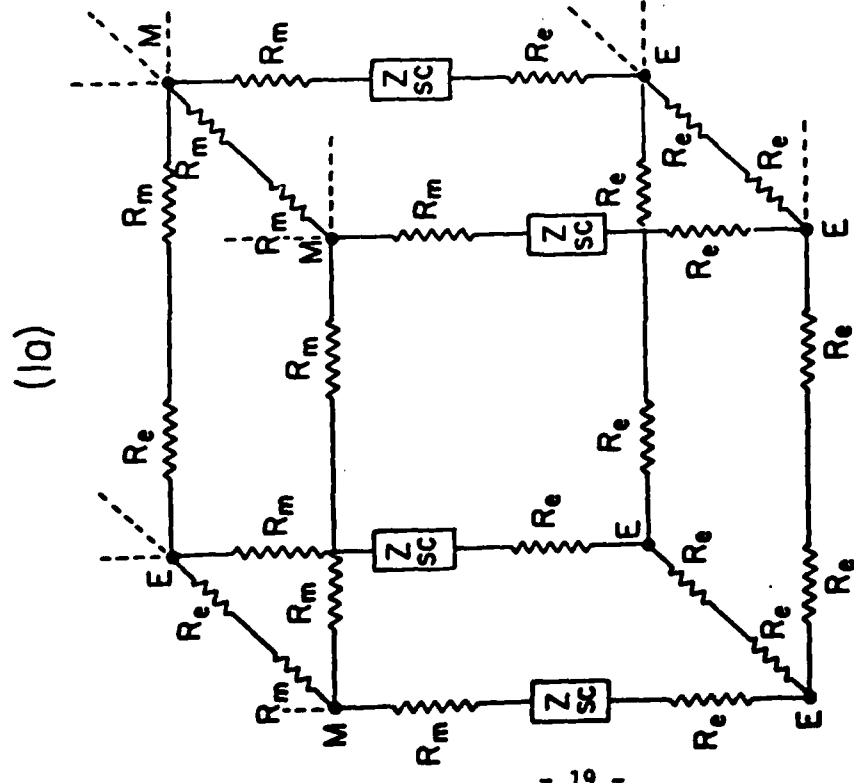
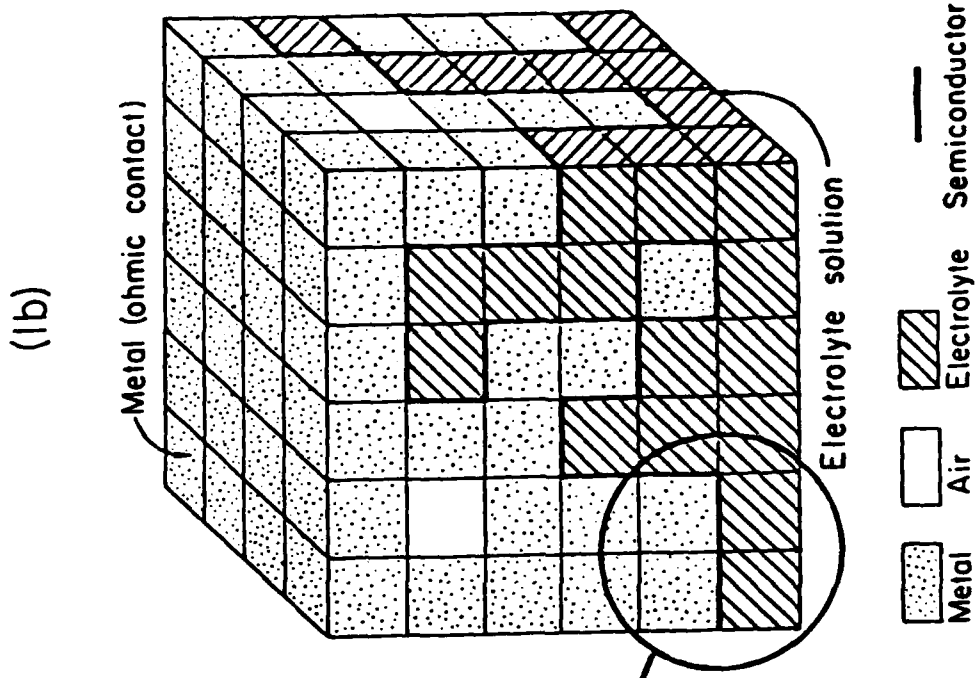


figure 1

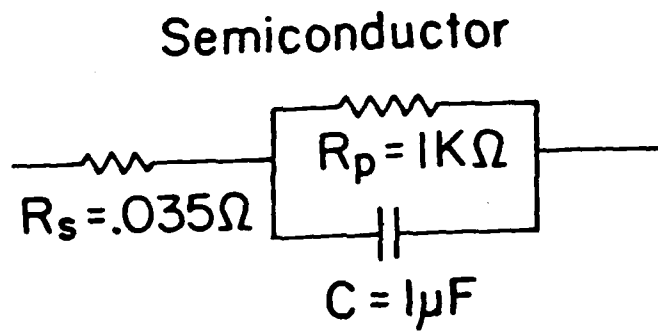
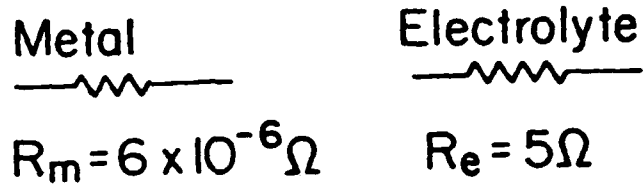


figure 2

LEVEL 7

LEVEL 6

LEVEL 5

LEVEL 4

LEVEL 3

LEVEL 2

LEVEL 1



- ELECTROLYTE
- METAL
- AIR

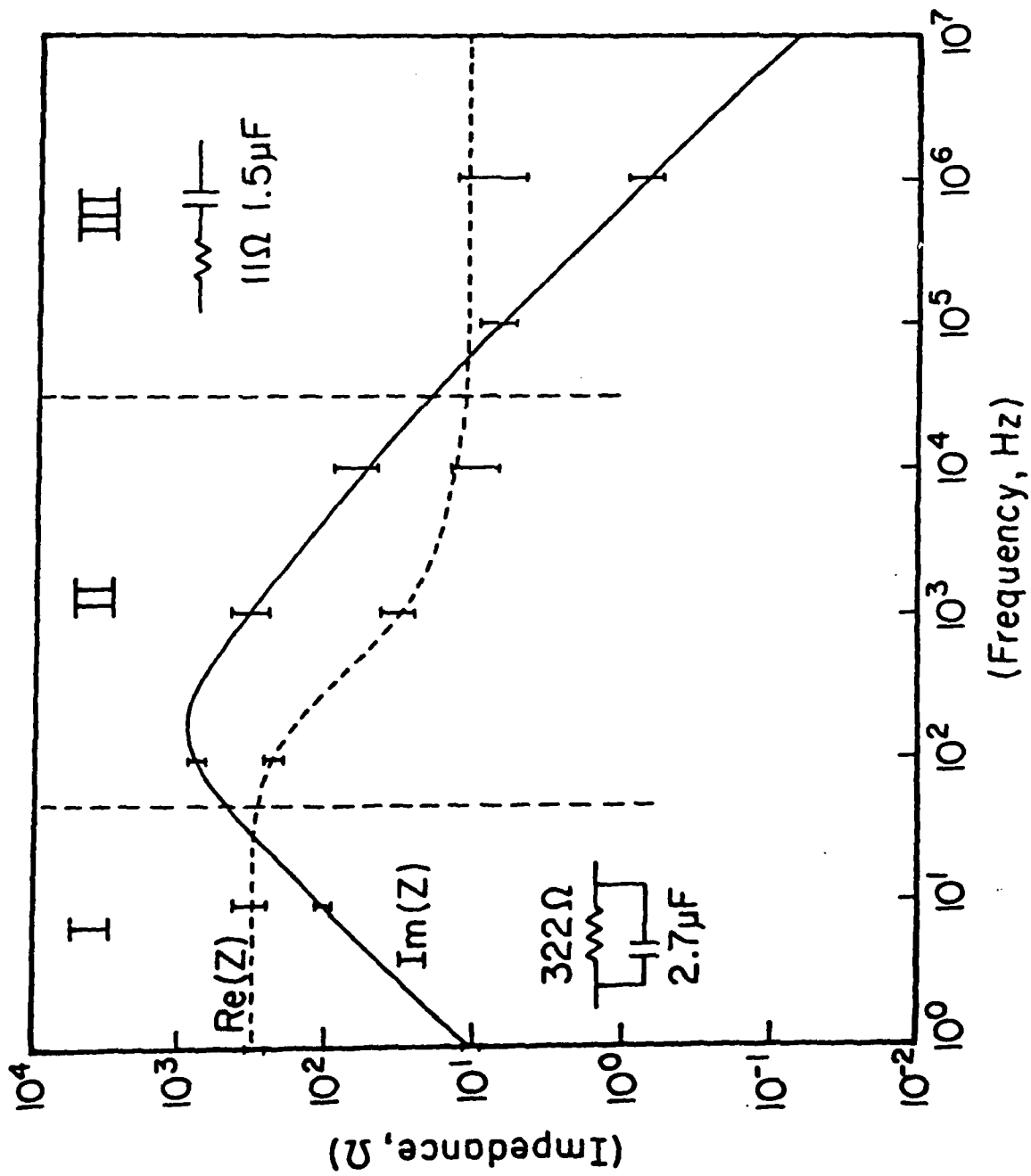


figure 4

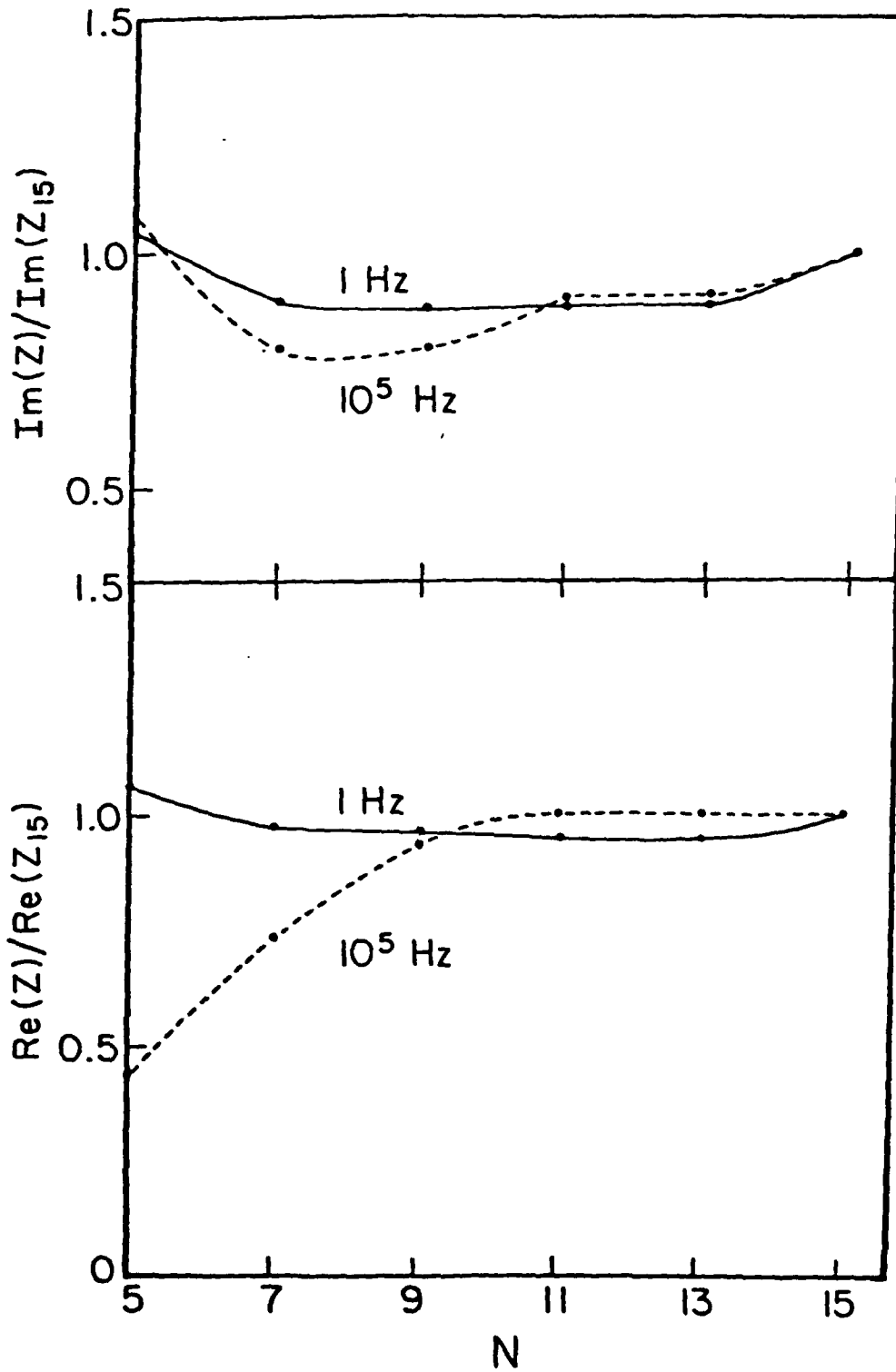
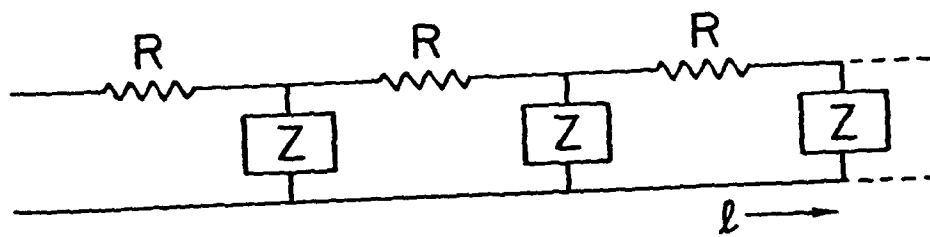
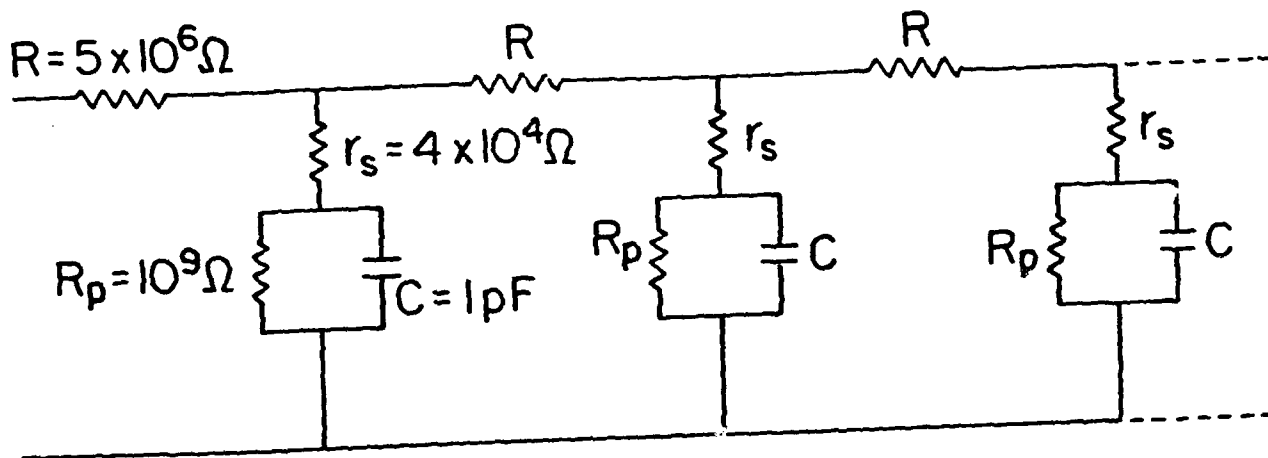


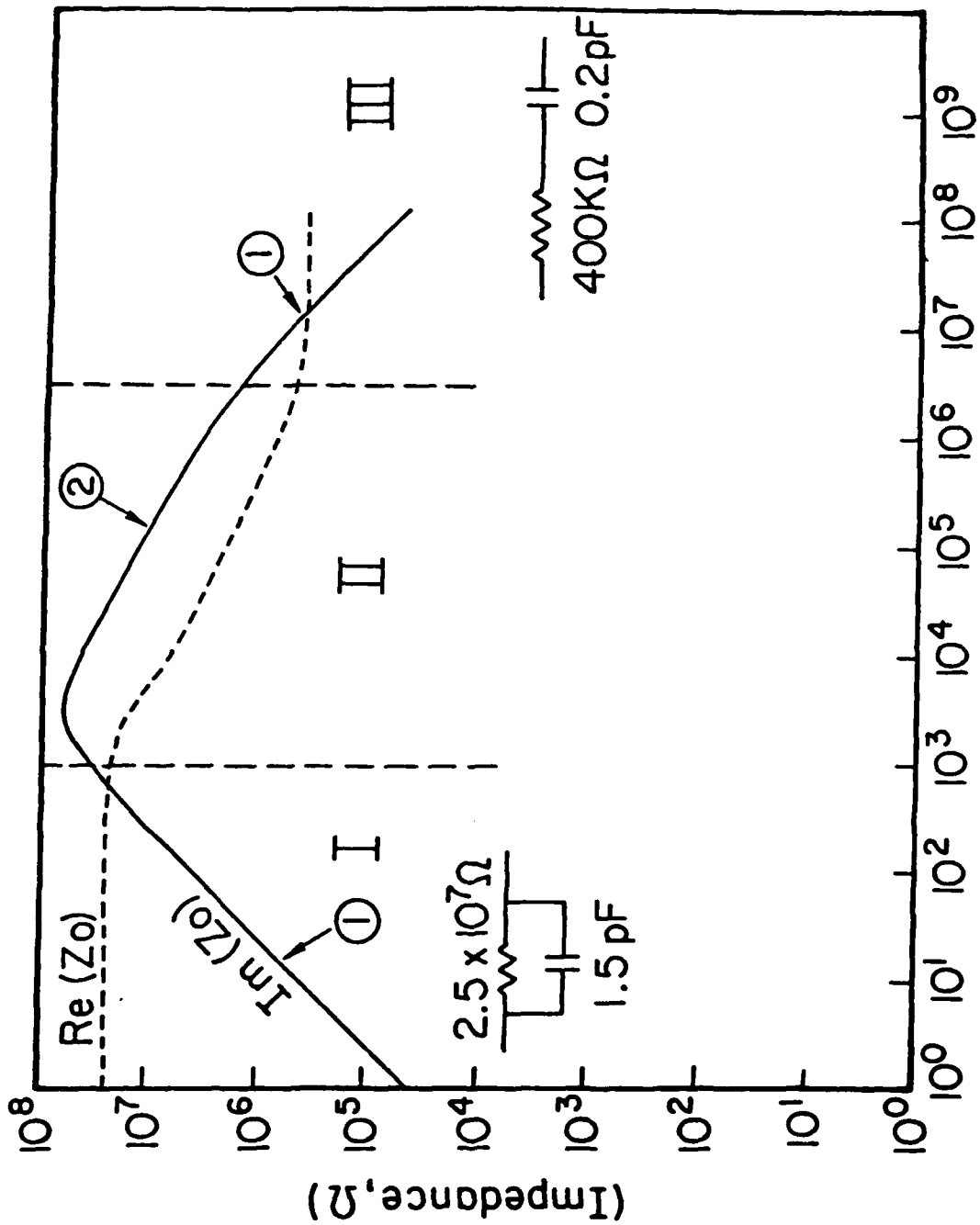
figure 5



(6a)



(6b)



(Frequency, Hz)

figure 7

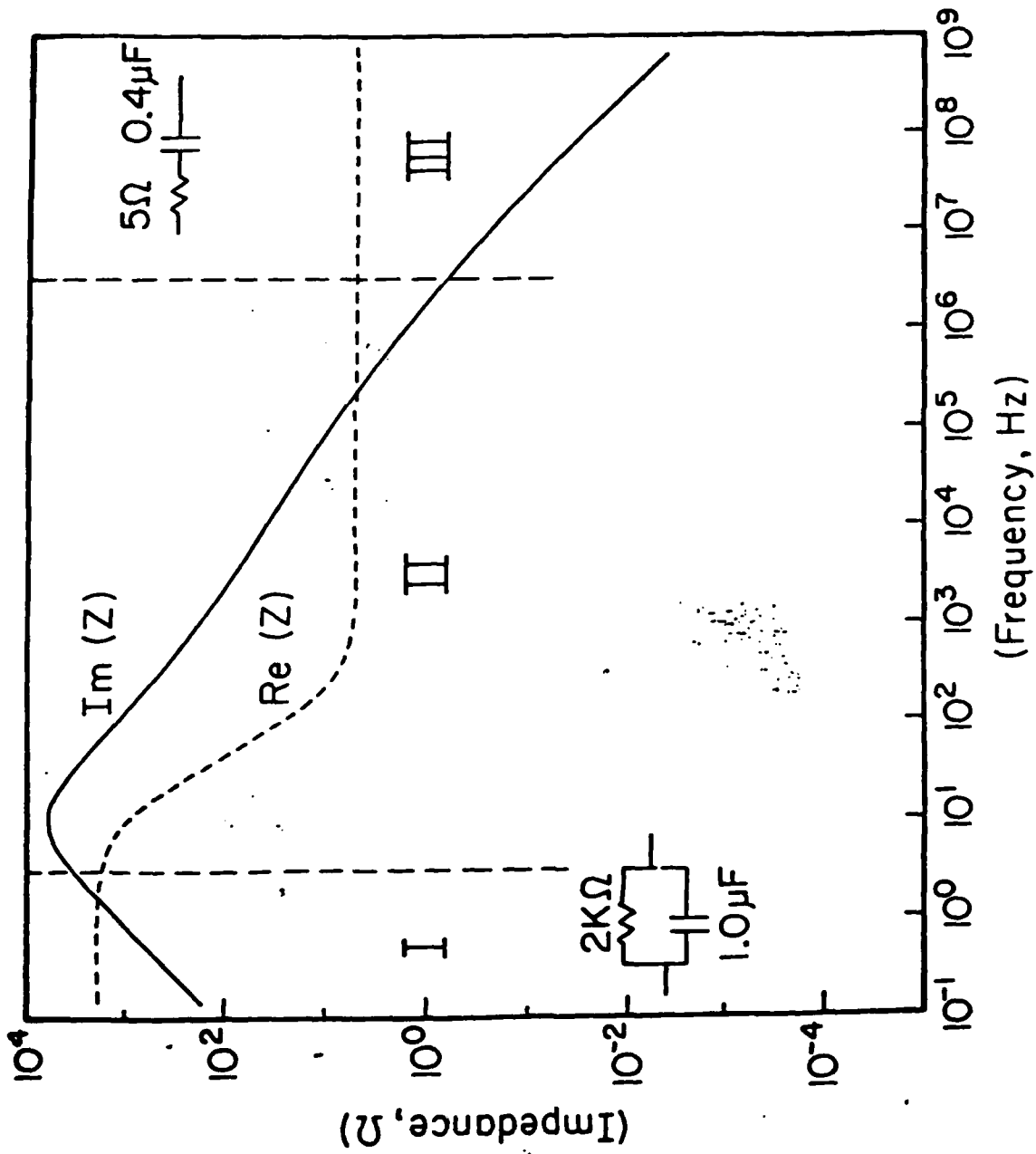


figure 8

TECHNICAL REPORT DISTRIBUTION LIST, GEN

	<u>No. Copies</u>		<u>No. Copies</u>
Office of Naval Research Attn: Code 413 800 N. Quincy Street Arlington, Virginia 22217	2	Naval Ocean Systems Center Attn: Technical Library San Diego, California 92152	1
ONR Pasadena Detachment Attn: Dr. R. J. Marcus 1030 East Green Street Pasadena, California 91106	1	Naval Weapons Center Attn: Dr. A. B. Amster Chemistry Division China Lake, California 93555	1
Commander, Naval Air Systems Command Attn: Code 310C (H. Rosenwasser) Washington, D.C. 20360	1	Scientific Advisor Commandant of the Marine Corps Code RD-1 Washington, D.C. 20380	1
Naval Civil Engineering Laboratory Attn: Dr. R. W. Drisko Port Hueneme, California 93401	1	Dean William Tolles Naval Postgraduate School Monterey, California 93940	1
Superintendent Chemistry Division, Code 6100 Naval Research Laboratory Washington, D.C. 20375	1	U.S. Army Research Office Attn: CRD-AA-IP P.O. Box 12211 Research Triangle Park, NC 27709	1
Defense Technical Information Center Building 5, Cameron Station Alexandria, Virginia 22314	12	Mr. Vincent Schaper DTNSRDC Code 2830 Annapolis, Maryland 21402	1
DTNSRDC Attn: Dr. G. Bosmajian Applied Chemistry Division Annapolis, Maryland 21401	1	Mr. John Boyle Materials Branch Naval Ship Engineering Center Philadelphia, Pennsylvania 19112	1
Naval Ocean Systems Center Attn: Dr. S. Yamamoto Marine Sciences Division San Diego, California 91232	1	Mr. A. M. Anzalone Administrative Librarian PLASTECH/ARRADCOM Bldg 3401 Dover, New Jersey 07801	1

TECHNICAL REPORT DISTRIBUTION LIST, 359

Dr. Paul Delahay
Department of Chemistry
New York University
New York, New York 10003

Dr. P. J. Hendra
Department of Chemistry
University of Southampton
Southampton SO9 5NH
United Kingdom

Dr. T. Katan
Lockheed Missiles and
Space Co., Inc.
P.O. Box 504
Sunnyvale, California 94088

Dr. D. N. Bennion
Department of Chemical Engineering
Brighma Young University
Provo, Utah 84602

Dr. R. A. Marcus
Department of Chemistry
California Institute of Technology
Pasadena, California 91125

Mr. Joseph McCartney
Code 7121
Naval Ocean Systems Center
San Diego, California 92152

Dr. J. J. Auburn
Bell Laboratories
Murray Hill, New Jersey 07974

Dr. Joseph Singer, Code 302-1
NASA-Lewis
21000 Brookpark Road
Cleveland, Ohio 44135

Dr. P. P. Schmidt
Department of Chemistry
Oakland University
Rochester, Michigan 48063

Dr. H. Richtol
Chemistry Department
Rensselaer Polytechnic Institute
Troy, New York 12181

Dr. E. Yeager
Department of Chemistry
Case Western Reserve University
Cleveland, Ohio 44106

Dr. C. E. Mueller
The Electrochemistry Branch
Naval Surface Weapons Center
White Oak Laboratory
Silver Spring, Maryland 20910

Dr. Sam Perone
Chemistry & Materials
Science Department
Lawrence Livermore National Lab.
Livermore, California 94550

Dr. Royce W. Murray
Department of Chemistry
University of North Carolina
Chapel Hill, North Carolina 27514

Dr. G. Goodman
Johnson Controls
5757 North Green Bay Avenue
Milwaukee, Wisconsin 53201

Dr. B. Brummer
EIC Incorporated
111 Chapel Street
Newton, Massachusetts 02158

Dr. Adam Heller
Bell Laboratories
Murray Hill, New Jersey 07974

Electrochimica Corporation
Attn: Technical Library
2485 Charleston Road
Mountain View, California 94040

Library
Duracell, Inc.
Burlington, Massachusetts 01803

Dr. A. B. Ellis
Chemistry Department
University of Wisconsin
Madison, Wisconsin 53706

TECHNICAL REPORT DISTRIBUTION LIST, 359

Dr. M. Wrighton
Chemistry Department
Massachusetts Institute
of Technology
Cambridge, Massachusetts 02139

Dr. B. Stanley Pons
Department of Chemistry
University of Utah
Salt Lake City, Utah 84112

Donald E. Mains
Naval Weapons Support Center
Electrochemical Power Sources Division
Crane, Indiana 47522

S. Ruby
DOE (STOR)
M.S. 68025 Forrestal Bldg.
Washington, D.C. 20595

Dr. A. J. Bard
Department of Chemistry
University of Texas
Austin, Texas 78712

Dr. Janet Osteryoung
Department of Chemistry
State University of New York
Buffalo, New York 14214

Dr. Donald W. Ernst
Naval Surface Weapons Center
Code R-33
White Oak Laboratory
Silver Spring, Maryland 20910

Mr. James R. Moden
Naval Underwater Systems Center
Code 3632
Newport, Rhode Island 02840

Dr. Bernard Spielvogel
U.S. Army Research Office
P.O. Box 12211
Research Triangle Park, NC 27709

Dr. William Ayers
ECD Inc.
P.O. Box 5357
North Branch, New Jersey 08876

Dr. M. M. Nicholson
Electronics Research Center
Rockwell International
3370 Miraloma Avenue
Anaheim, California

Dr. Michael J. Weaver
Department of Chemistry
Purdue University
West Lafayette, Indiana 47907

Dr. R. David Rauh
EIC Corporation
111 Chapel Street
Newton, Massachusetts 02158

Dr. Aaron Wold
Department of Chemistry
Brown University
Providence, Rhode Island 02192

Dr. Martin Fleischmann
Department of Chemistry
University of Southampton
Southampton SO9 5NH ENGLAND

Dr. R. A. Osteryoung
Department of Chemistry
State University of New York
Buffalo, New York 14214

Dr. Denton Elliott
Air Force Office of Scientific
Research
Bolling AFB
Washington, D.C. 20332

Dr. R. Nowak
Naval Research Laboratory
Code 6130
Washington, D.C. 20375

Dr. D. F. Shriver
Department of Chemistry
Northwestern University
Evanston, Illinois 60201

Dr. Aaron Fletcher
Naval Weapons Center
Code 3852
China Lake, California 93555

TECHNICAL REPORT DISTRIBUTION LIST, 359

Dr. David Aikens
Chemistry Department
Rensselaer Polytechnic Institute
Troy, New York 12181

Dr. A. P. B. Lever
Chemistry Department
York University
Downsview, Ontario M3J1P3

Dr. Stanislaw Szpak
Naval Ocean Systems Center
Code 6343, Bayside
San Diego, California 95152

Dr. Gregory Farrington
Department of Materials Science
and Engineering
University of Pennsylvania
Philadelphia, Pennsylvania 19104

M. L. Robertson
Manager, Electrochemical
and Power Sources Division
Naval Weapons Support Center
Crane, Indiana 47522

Dr. T. Marks
Department of Chemistry
Northwestern University
Evanston, Illinois 60201

Dr. Micha Tomkiewicz
Department of Physics
Brooklyn College
Brooklyn, New York 11210

Dr. Lesser Blum
Department of Physics
University of Puerto Rico
Rio Piedras, Puerto Rico 00931

Dr. Joseph Gordon, II
IBM Corporation
K33/281
5600 Cottle Road
San Jose, California 95193

Dr. D. H. Whitmore
Department of Materials Science
Northwestern University
Evanston, Illinois 60201

Dr. Alan Bewick
Department of Chemistry
The University of Southampton
Southampton, SO9 5NH ENGLAND

Dr. E. Anderson
NAVSEA-56Z33 NC #4
2541 Jefferson Davis Highway
Arlington, Virginia 20362

Dr. Bruce Dunn
Department of Engineering &
Applied Science
University of California
Los Angeles, California 90024

Dr. Elton Cairns
Energy & Environment Division
Lawrence Berkeley Laboratory
University of California
Berkeley, California 94720

Dr. D. Cipris
Allied Corporation
P.O. Box 3000R
Morristown, New Jersey 07960

Dr. M. Philpott
IBM Corporation
5600 Cottle Road
San Jose, California 95193

Dr. Donald Sandstrom
Department of Physics
Washington State University
Pullman, Washington 99164

Dr. Carl Kannewurf
Department of Electrical Engineering
and Computer Science
Northwestern University
Evanston, Illinois 60201

TECHNICAL REPORT DISTRIBUTION LIST, 359

Dr. Robert Somoano
Jet Propulsion Laboratory
California Institute of Technology
Pasadena, California 91103

Dr. Johann A. Joebstl
USA Mobility Equipment R&D Command
DRDME-EC
Fort Belvoir, Virginia 22060

Dr. Judith H. Ambrus
NASA Headquarters
M.S. RTS-6
Washington, D.C. 20546

Dr. Albert R. Landgrebe
U.S. Department of Energy
M.S. 68025 Forrestal Building
Washington, D.C. 20595

Dr. J. J. Brophy
Department of Physics
University of Utah
Salt Lake City, Utah 84112

Dr. Charles Martin
Department of Chemistry
Texas A&M University
College Station, Texas 77843

Dr. H. Tachikawa
Department of Chemistry
Jackson State University
Jackson, Mississippi 39217

Dr. Theodore Beck
Electrochemical Technology Corp.
3935 Leary Way N.W.
Seattle, Washington 98107

Dr. Farrell Lytle
Boeing Engineering and
Construction Engineers
P.O. Box 3707
Seattle, Washington 98124

Dr. Robert Gotscholl
U.S. Department of Energy
MS G-226
Washington, D.C. 20545

Dr. Edward Fletcher
Department of Mechanical Engineering
University of Minnesota
Minneapolis, Minnesota 55455

Dr. John Fontanella
Department of Physics
U.S. Naval Academy
Annapolis, Maryland 21402

Dr. Martha Greenblatt
Department of Chemistry
Rutgers University
New Brunswick, New Jersey 08903

Dr. John Wasson
Syntheco, Inc.
Rte 6 - Industrial Pike Road
Gastonia, North Carolina 28052

Dr. Walter Roth
Department of Physics
State University of New York
Albany, New York 12222

Dr. Anthony Sammells
Eltron Research Inc.
710 E. Ogden Avenue #108
Naperville, Illinois 60540

Dr. W. M. Risen
Department of Chemistry
Brown University
Providence, Rhode Island 02192

Dr. C. A. Angell
Department of Chemistry
Purdue University
West Lafayette, Indiana 47907

Dr. Thomas Davis
Polymer Science and Standards
Division
National Bureau of Standards
Washington, D.C. 20234

ATE
LMED
8